Figure S1

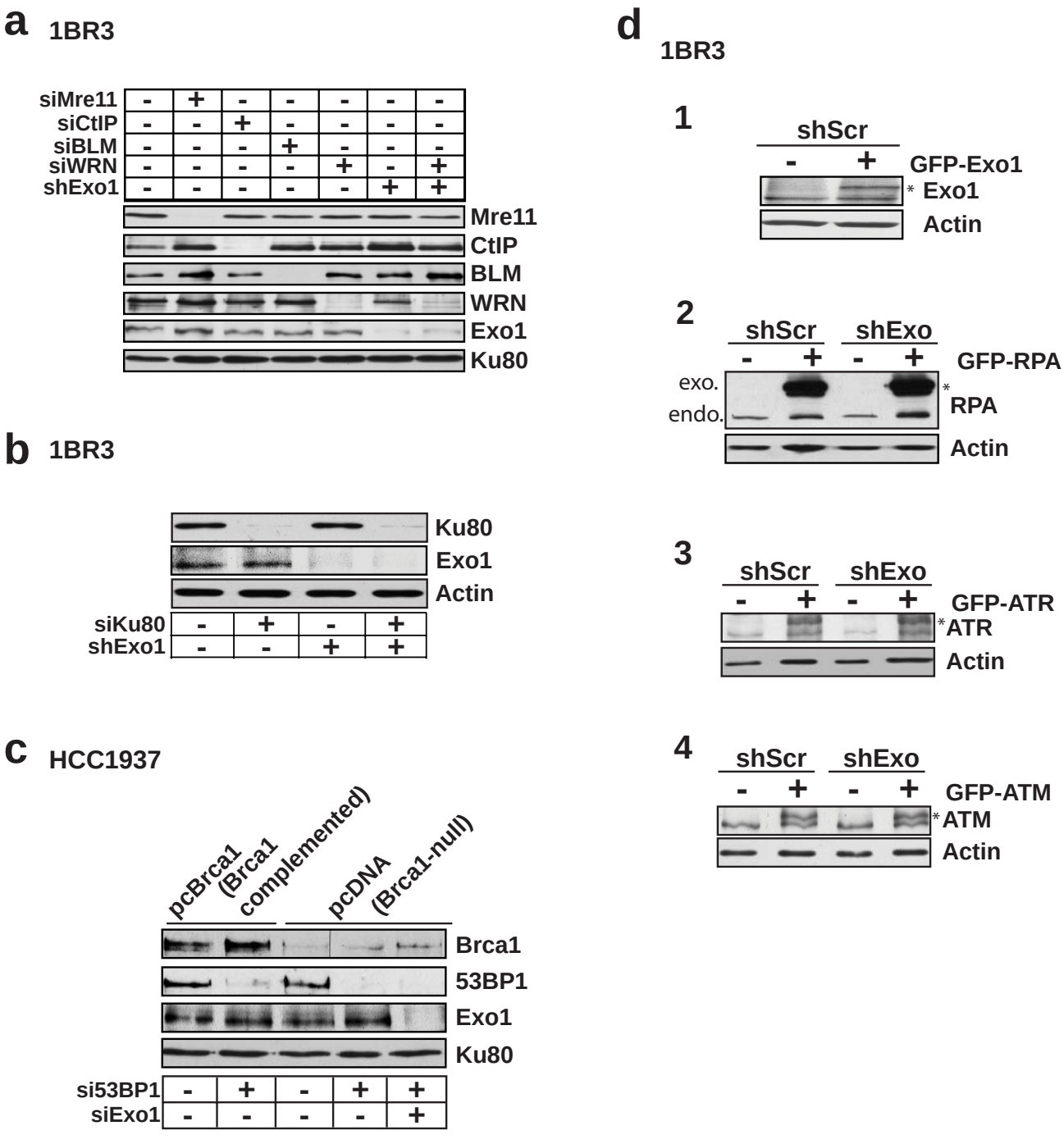
a
1BR3
siMre11
siCtIP
siBLM
siWRN
shExo1
Mre11
CtIP
BLM
WRN
Exo1
Ku80
b
1BR3
Ku80
Exo1
Actin
siKu80
shExo1
c
HCC1937
pcBrca1 (Brca1 complemented)
pcDNA (Brca1-null)
Brca1
53BP1
Exo1
Ku80
si53BP1
siExo1
d
1BR3
1
shScr
GFP-Exo1
Exo1
Actin
2
shScr
shExo
GFP-RPA
exo.
endo.
RPA
Actin
3
shScr
shExo
GFP-ATR
ATR
Actin
4
shScr
shExo
GFP-ATM
ATM
Actin

Figure S2

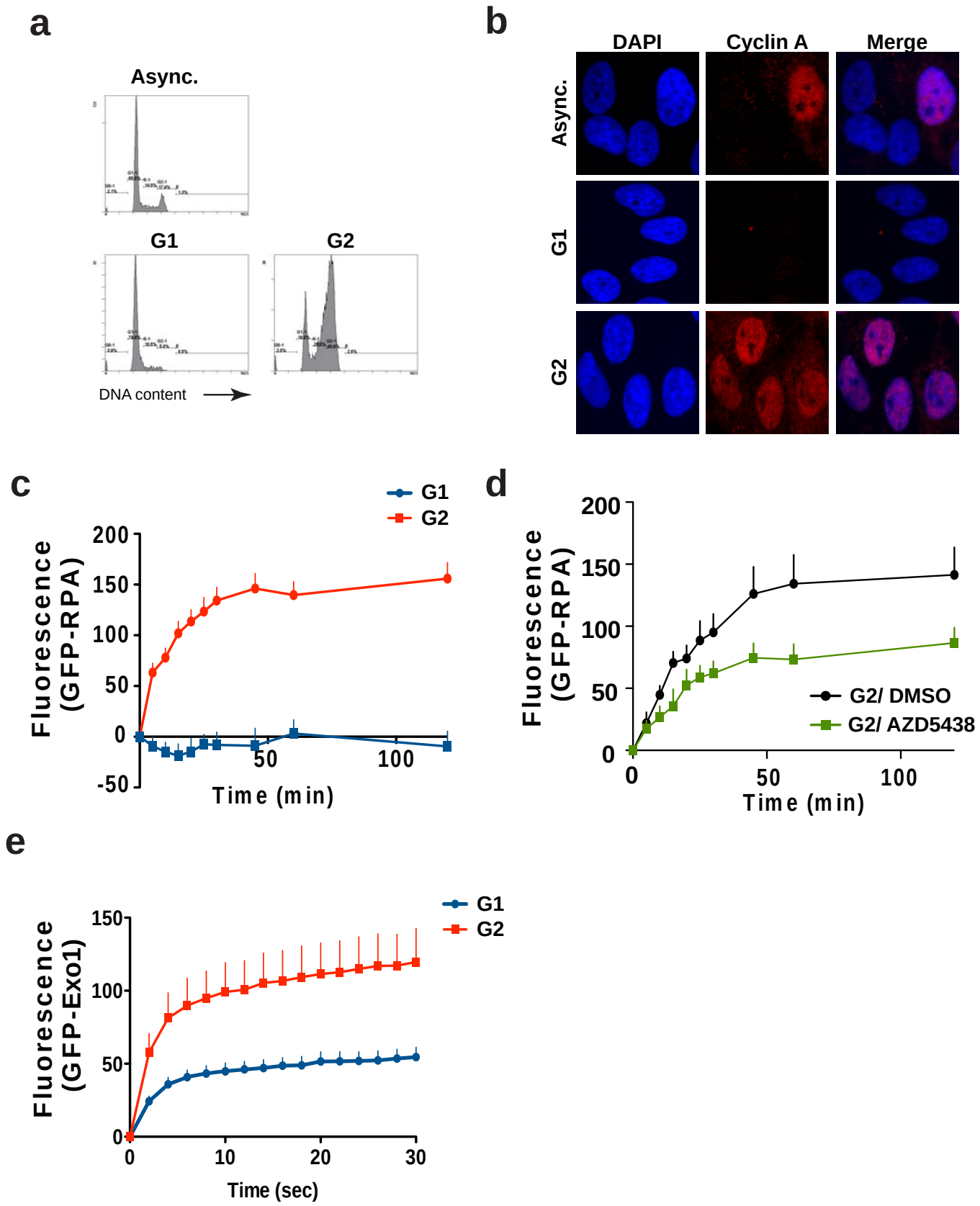
a
Async.
G1
G2
DNA content
b
DAPI
Cyclin A
Merge
Async.
G1
G2
c
G1
G2
Fluorescence (GFP-RPA)
200
150
100
50
0
-50
50
100
Time (min)
d
Fluorescence (GFP-RPA)
200
150
100
50
0
0
50
100
Time (min)
G2/ DMSO
G2/ AZD5438
e
Fluorescence (GFP-Exo1)
150
100
50
0
0
10
20
30
Time (sec)
G1
G2

Figure S3

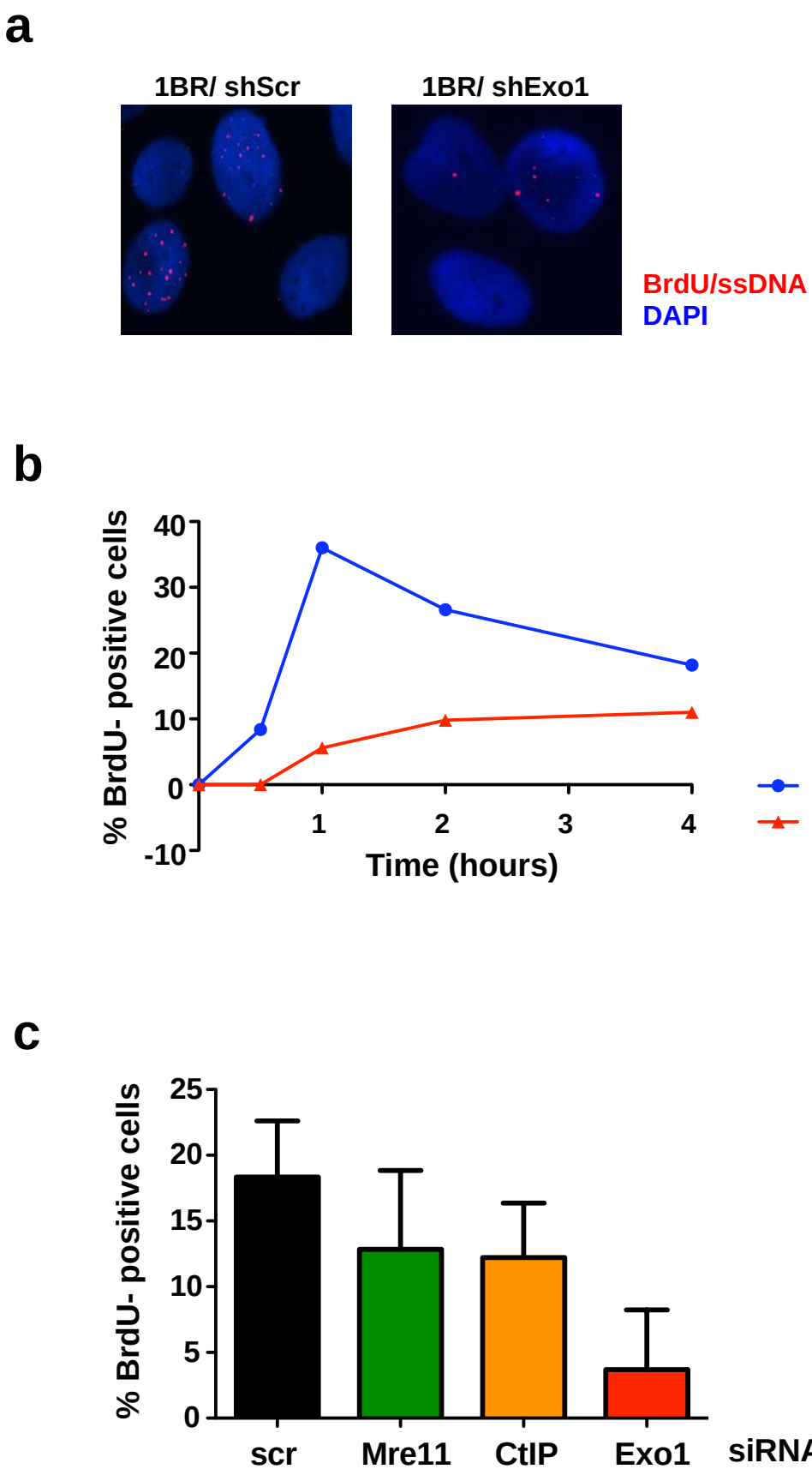
a
1BR/ shScr
1BR/ shExo1
BrdU/ssDNA
DAPI
b
% BrdU- positive cells
40
30
20
10
0
-10
1
2
3
4
Time (hours)
1BR/shScr
1BR/shExo1
c
% BrdU- positive cells
25
20
15
10
5
0
scr
Mre11
CtIP
Exo1
siRNA

Figure S4

a

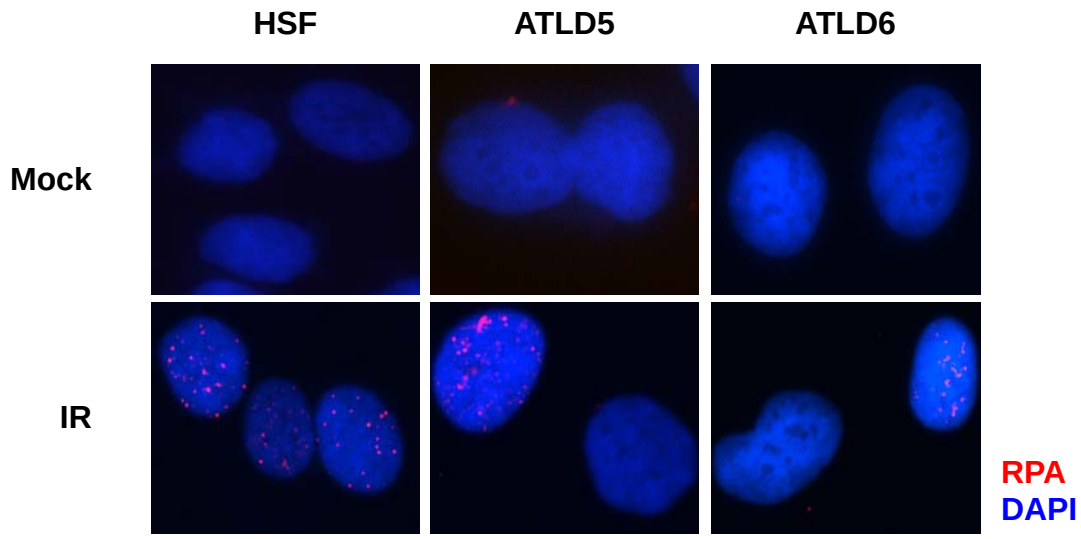
HSF
ATLD5
ATLD6
Mock
IR
RPA
DAPI

b

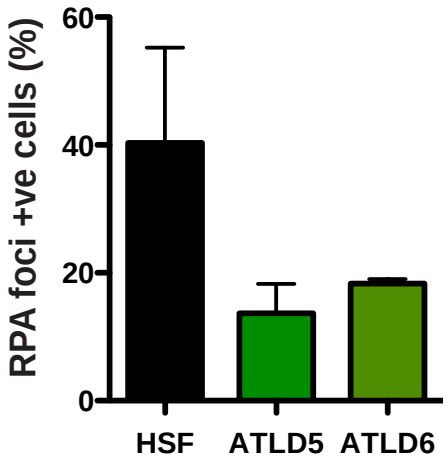
RPA foci +ve cells (%)
60
40
20
0
HSF
ATLD5
ATLD6

Figure S5

a

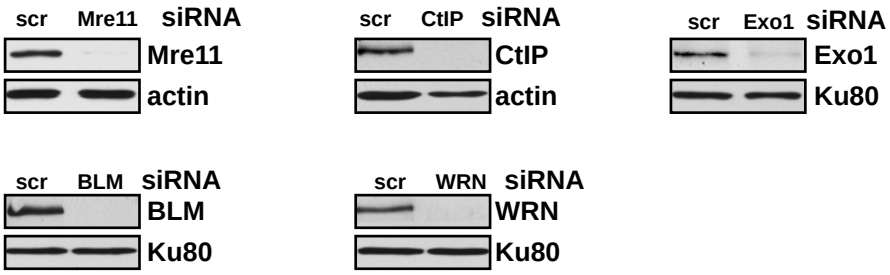

b

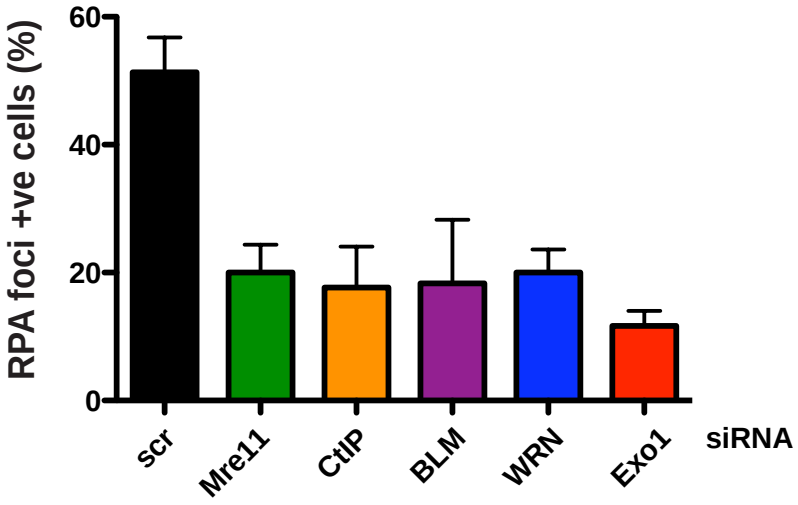

c

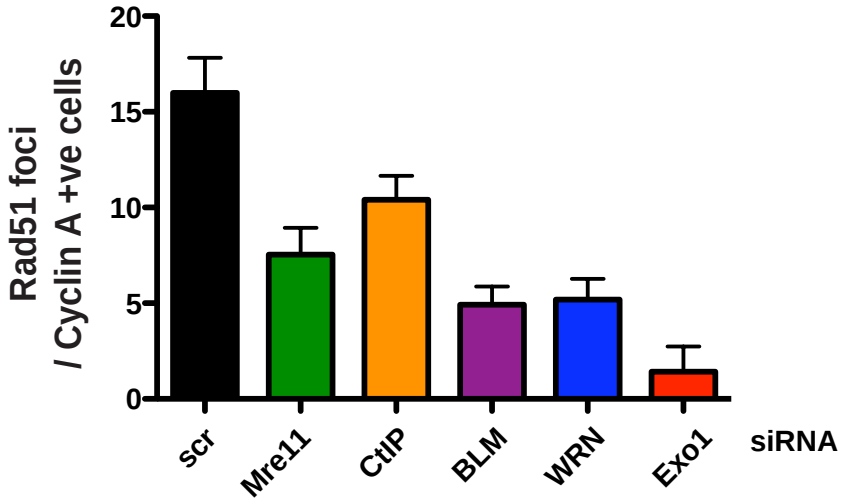

Tomimatsu et al; Supplement

Figure S6

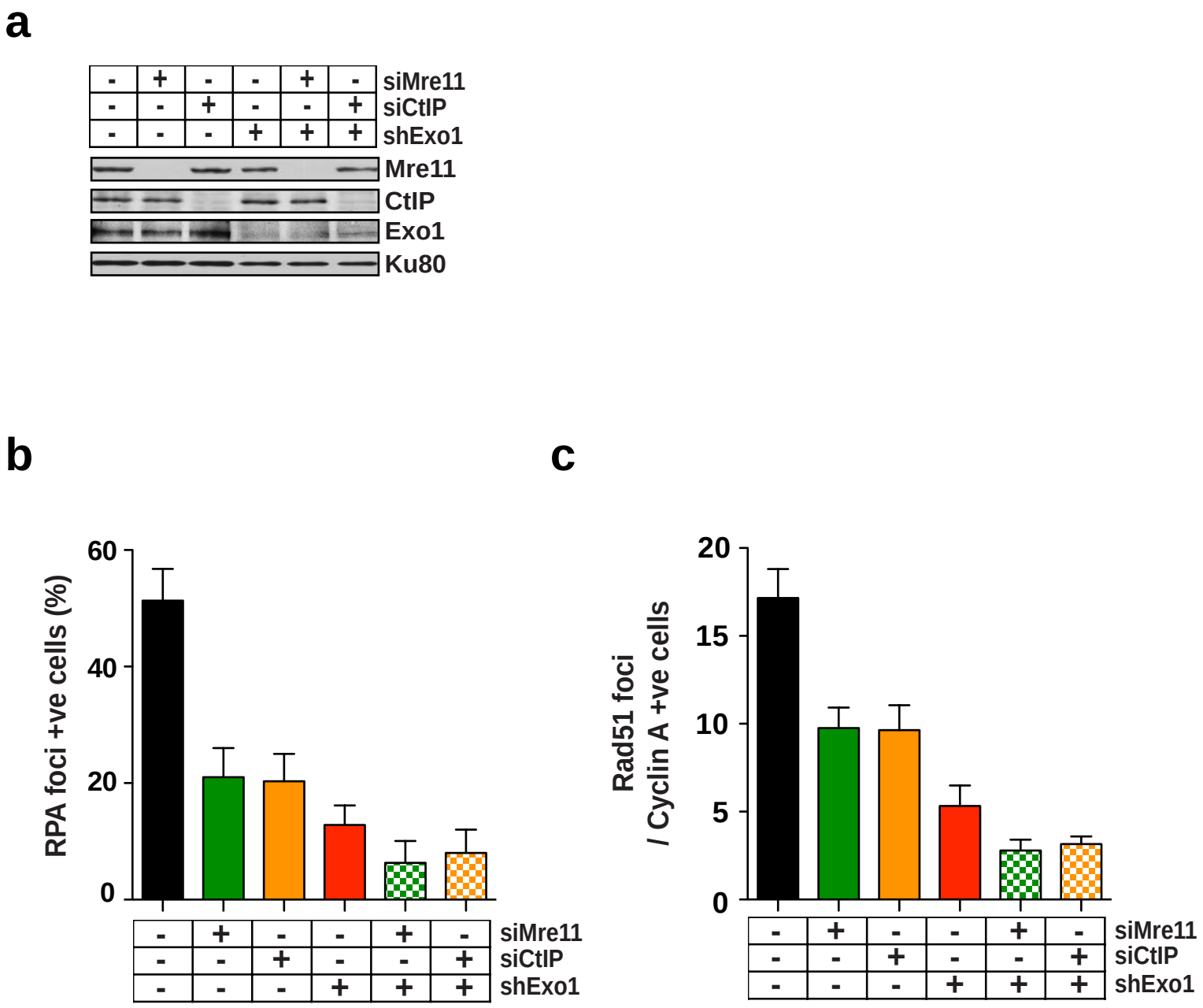

Tomimatsu et al; Supplement

Figure S7

a

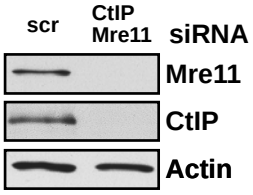

b

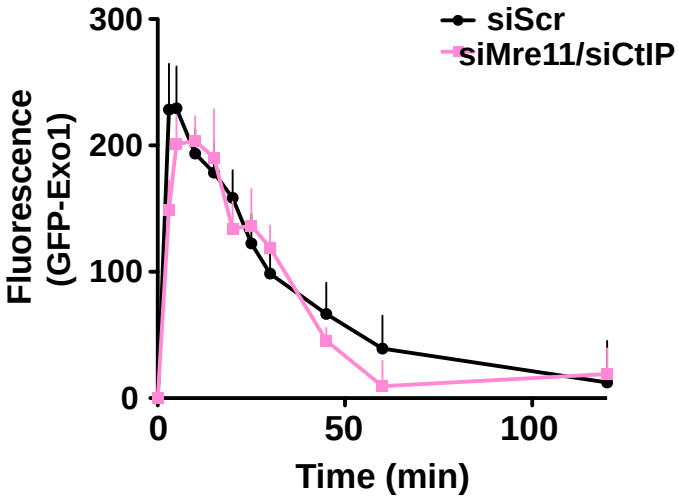

Tomimatsu et al; Supplement

Figure S8

a

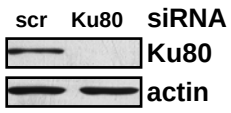

b

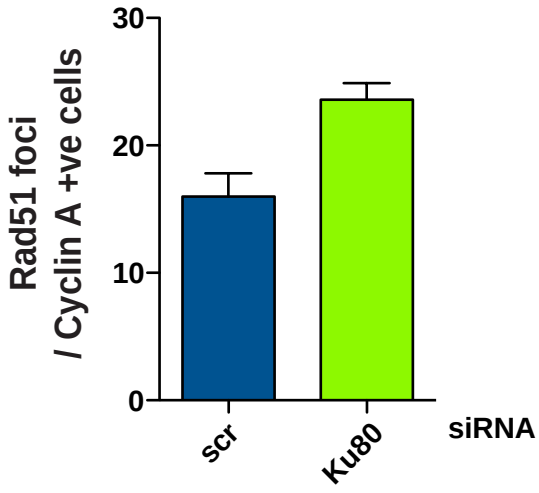

Figure S9

a

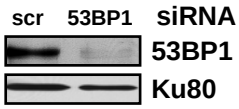
scr
53BP1
siRNA
53BP1
Ku80

b

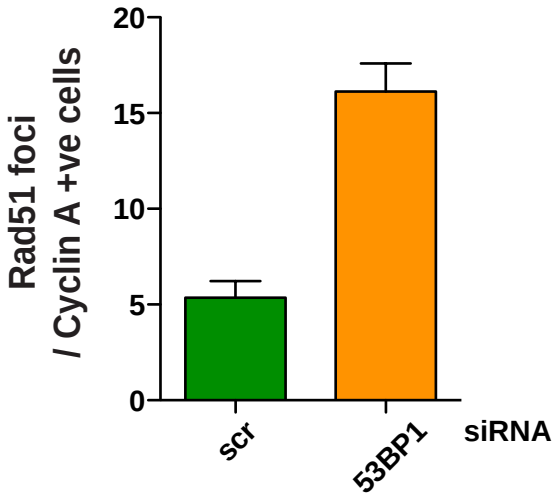
Rad51 foci
/ Cyclin A +ve cells
20
15
10
5
0
scr
53BP1
siRNA

Figure S10

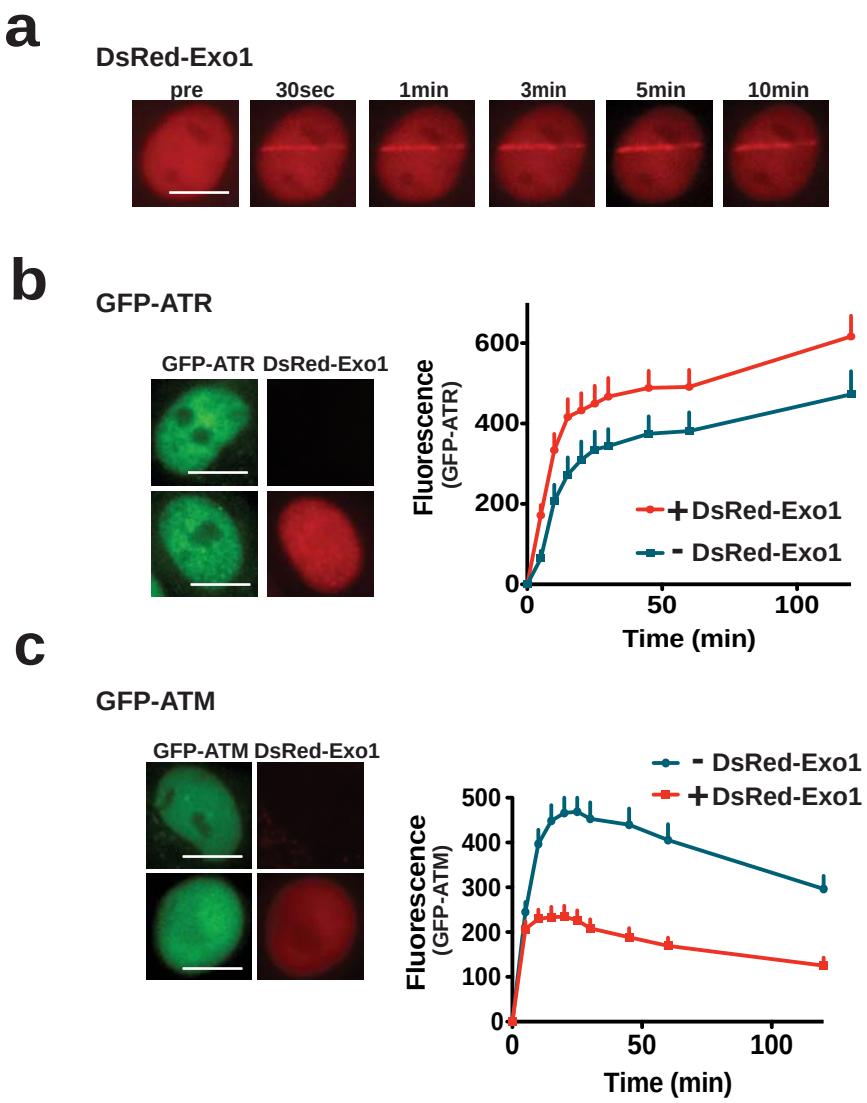
a
DsRed-Exo1
pre
30sec
1min
3min
5min
10min
b
GFP-ATR
GFP-ATR DsRed-Exo1
Fluorescence (GFP-ATR)
600
400
200
0
0
50
100
Time (min)
+DsRed-Exo1
-DsRed-Exo1
c
GFP-ATM
GFP-ATM DsRed-Exo1
Fluorescence (GFP-ATM)
500
400
300
200
100
0
0
50
100
Time (min)
-DsRed-Exo1
+DsRed-Exo1

Tomimatsu et al; Supplement

Table 1 siRNAs used in figures 1-4

	Vendor	Cat No
Scr shRNA	Santacruz	sc-108060
Scr siRNA	Invitrogen	12935-300
Mre11 siRNA	Invitrogen	HSS142961
CtIP siRNA	Invitrogen	HSS109108
Exo1 shRNA	Santacruz	sc-44880-SH
Exo1 siRNA	Invitrogen	HSS113557
BLM siRNA	Invitrogen	HSS101024
WRN siRNA	Invitrogen	HSS111385
Ku80 siRNA	Invitrogen	HSS111425
53BP1 siRNA	Invitrogen	HSS110908

Tomimatsu et al; Supplement

Table 2 siRNAs used in supplemental figures S5, S8, S9

	Vendor	**Cat No /sequence**
Mre11 siRNA	Invitrogen (custom synthesis)	AGUUGAUCUCUUCUCCUGU(dT)(dT)
CtIP siRNA	Invitrogen	HSS109109
Exo1 siRNA	Invitrogen	HSS113558
BLM siRNA	Invitrogen	HSS101023
WRN siRNA	Invitrogen	HSS187703
Ku80 siRNA	Invitrogen	HSS111426
53BP1 siRNA	Invitrogen	HSS110909

Tomimatsu et al; Legends to Supplemental Figures

Figure S1 (a) Knockdown of Exo1, Mre11, CtIP, BLM, or WRN in 1BR3 cells was verified by Western blotting with relevant antibodies. The siRNAs used for these knockdowns are listed in supplemental **Table 1.** **(b)** Knockdown of Ku80 and/or Exo1 in 1BR3 cells was verified by Western blotting with relevant antibodies. **(c)** Knockdown of Exo1 and/or 53BP1 in Brca1-null or Brca1-complemented HCC1937 cells was verified by Western blotting with relevant antibodies.**(d)** Expression of GFP-tagged **(1)** Exo1, **(2)** RPA, **(3)** ATR, or **(4)** ATM in 1BR3 cells was verified by Western blotting with relevant antibodies (the GFP-protein bands are marked by asterisks).

Figure S2 (a) In order to examine cell cycle-dependency of GFP-RPA or GFP-Exo1 recruitment to laser-induced breaks, 1BR3 cells were synchronized in G1 or G2 phases of the cell cycle as described [1]. Synchronization was confirmed by single parameter flow cytometry. **(b)** Synchronization was re-confirmed by staining cells synchronized on cover slips with anti-Cyclin A antibody (green) which stains cells in S/G2 phases of the cell cycle [2]. Nuclei are stained with DAPI (blue). **(c)** GFP-RPA expressing cells (Fig. S1d) synchronized in G1 or G2 were laser micro-irradiated and kinetics of RPA accumulation plotted. **(d)** G2 synchronized cells were pre-treated with the CDK inhibitor AZD5438 (Selleck; 1 μM) [3] or with DMSO as a control before laser micro-irradiation and live-cell imaging. Please note complete absence of RPA accumulation in G1 cells and attenuation of RPA accumulation upon CDK inhibition, confirming that GFP-RPA recruitment kinetics reflects physiologically relevant DNA end resection. **(e)** GFP-Exo1-expressing cells (Fig. S1d) synchronized in G1 or G2 were laser micro-irradiated and kinetics of

Exo1 accumulation plotted as described **[4]**. Please note significantly reduced accumulation of Exo1 in G1 cells (G1 accumulation might indicate a possible role of Exo1 in minimal DNA-end processing during NHEJ or alt NHEJ.) All laser experiments involving Exo1 recruitment were carried out in cells synchronized in G2 in order to quantify Exo1 recruitment in the context of HR-relevant resection.

Figure S3 (a) In order to further confirm that GFP-RPA accumulation kinetics reflects physiologically-relevant resection, the generation of ssDNA in gamma ray-irradiated 1BR3 cells was directly quantified by staining for 5-bromo-2-deoxyuridine (BrdU) foci as described [5]. Briefly, 1BR3 cells were grown in the presence of 10 μM BrdU (Sigma) for 16 hours, irradiated with 10 Gy of gamma rays, fixed at the indicated times,and immunofluorescence stained with an anti-BrdU antibody (BD Bioscience) under nondenaturing conditions (in order to detect BrdU incorporated into ssDNA). Representative images are shown of IR-induced ssDNA foci in 1BR3 cells with or without Exo1 depletion at 1 hour post-irradiation. Nuclei are stained with DAPI. **(b)** Percentage of cells with > 10 BrdU/ssDNA foci (*y* axis) are plotted against times post-irradiation (*x* axis) after subtracting background (percent BrdU-positive cells in mock-irradiated cultures). Please note peak levels of ssDNA foci at 1 hour post-IR which is similar to time taken for peak GFP-RPA accumulation in live-cell experiments (Fig. 1a). Also note ablation of ssDNA foci upon Exo1 knockdown, confirming that Exo1 plays a major role in DNA end resection in human cells. **(c)** Percentage of cells with > 10 BrdU/ssDNA foci at 1 hour post-irradiation are plotted for 1BR3 cells with siRNA-mediated knockdown of Mre11, CtIP, or Exo1 as indicated.

Figure S4 (a) Representative image of gamma-irradiated wild type human skin fibroblasts (HSF) [1] or Mre11-deficient ATLD cells [6] immunnostained with anti-RPA antibody (red) after 3 hours. Nuclei are stained with DAPI (blue). **(b)** Percentages of RPA-positive cells (10 or more foci) are plotted for HSF and ATLD cells.

Figure S5 (a) To rule out any "off-target" effect of the siRNAs used in Fig. 1 (Supplement; Table 1), Mre11, CtIP, Exo1, BLM, or WRN were depleted in 1BR3 cells with a second set of different siRNAs (Supplement; Table 2) and IR-induced **(b)** RPA and **(c)** Rad51 foci were quantified.

Figure S6 (a) Knockdown of Mre11, CtIP, and/orExo1 in 1BR3 cells was verified by Western blotting with relevant antibodies. **(b)** Percentages of RPA-positive cells (10 or more foci) are plotted for irradiated 1BR3 cells with depletion of Mre11, CtIP, Exo1, Mre11/Exo1, or CtIP/Exo1. **(c)** Average numbers of Rad51 foci for irradiated Cyclin A-positive (S/G2) nuclei are plotted for 1BR3 cells with depletion of Mre11, CtIP, Exo1, Mre11/Exo1, or CtIP/Exo1.

Figure S7 (a) Mre11 and CtIP were co-depleted in 1BR3 cells and **(b)** kinetics of recruitment of GFP-Exo1 at DSBs induced by laser micro-irradiation was quantified as described [4].

Figure S8 (a) (a) To rule out any "off-target" effect of the Ku80 siRNA used in Fig. 2 (Supplement; Table 1), Ku80 was depleted in 1BR3 cells with a different siRNA (Supplement; Table 2) and **(b)** IR-induced Rad51 foci were quantified.

Figure S9 (a) To rule out any "off-target" effect of the 53BP1 siRNAs used in Fig. 3 (Supplement; Table 1), 53BP1 was depleted in HCC1937 cells with a different siRNA (Supplement; Table 2) and **(b)** IR-induced Rad51 foci were quantified.

Figure S10 (a) 1BR3 cells were transfected with a pLenti6.3-DsRed-Exo1construct and rapid accumulation of DsRed-Exo1 to the sites of laser micro-irradiation was confirmed to ensure that the ectopically-expressed Exo1 is functional. The pLenti6.3-DsRed-Exo1 construct (expressing N-terminally tagged Exo1) was generated by ligating the DsRed cDNA upstream and in-frame with ExoI cDNA contained in a pDONR221 vector. The ligation product was then recombined into pLenti6.3 (Invitrogen) to yield the final expression vector. Plots show the recruitment of **(b)** GFP-ATR or **(c)** GFP-ATM to the sites of DSBs induced by laser micro-irradiation in wild type 1BR3 cells expressing DsRed-Exo1 (red plots) *versus* cells not expressing DsRed-Exo1 (blue plots). Representative images show co-expression of GFP-ATR or GFP-ATM (green) with DsRed-Exo1 (red) in nuclei of 1BR3 cells. Scale bars, 10 μm. Please note that ectopic expression of Exo1 augments ATR recruitment and attenuates ATM recruitment to laser-induced DSBs.

References

[1] N. Tomimatsu, B. Mukherjee, S. Burma, Distinct roles of ATR and DNA-PKcs in triggering DNA damage responses in ATM-deficient cells, EMBO Rep, (2009).

[2] S. Bekker-Jensen, C. Lukas, R. Kitagawa, F. Melander, M.B. Kastan, J. Bartek, J. Lukas, Spatial organization of the mammalian genome surveillance machinery in response to DNA strand breaks, J Cell Biol, 173 (2006) 195-206.

[3] K.F. Byth, A. Thomas, G. Hughes, C. Forder, A. McGregor, C. Geh, S. Oakes, C. Green, M. Walker, N. Newcombe, S. Green, J. Growcott, A. Barker, R.W. Wilkinson, AZD5438, a potent oral inhibitor of cyclin-dependent kinases 1, 2, and 9, leads to pharmacodynamic changes and potent antitumor effects in human tumor xenografts, Mol Cancer Ther, 8 (2009) 1856-1866.

[4] E. Bolderson, N. Tomimatsu, D.J. Richard, D. Boucher, R. Kumar, T.K. Pandita, S. Burma, K.K. Khanna, Phosphorylation of Exo1 modulates homologous recombination repair of DNA double-strand breaks, Nucleic Acids Res, (2009).

[5] Y. Hu, R. Scully, B. Sobhian, A. Xie, E. Shestakova, D.M. Livingston, RAP80-directed tuning of BRCA1 homologous recombination function at ionizing radiation-induced nuclear foci, Genes Dev, 25 (2011) 685-700.

[6] D. Delia, M. Piane, G. Buscemi, C. Savio, S. Palmeri, P. Lulli, L. Carlessi, E. Fontanella, L. Chessa, MRE11 mutations and impaired ATM-dependent responses in an Italian family with ataxia-telangiectasia-like disorder, Hum Mol Genet, 13 (2004) 2155-2163.